Flexible Piezoelectric Energy Harvesting Circuit with Printable Supercapacitor and Diodes

Juho Pörhönen, Satu Rajala, Suvi Lehtimäki, and Sampo Tuukkanen

***Abstract*—We report a flexible energy harvesting circuit fabricated by roll-to-roll compatible, solution-processable methods. The circuit incorporates a supercapacitor fabricated from a viscous carbon nanotube (CNT) dispersion, printed Schottky diodes and a piezoelectric element. Used low-temperature materials enabled component integration on poly(ethylene terephthalate) (PET) substrate. The supercapacitor was built with a paper separator and an aqueous NaCl electrolyte. Together with carbon based electrodes, these materials translated into a disposable and environmentally safe electronic device. The energy harvested from mechanical movement was used to drive a commercial electrochromic display.**

***Index Terms*— energy harvesting, piezoelectricity, supercapacitor, printed electronics**

I. Introduction

PRINTED and organic electronics has attracted much attention during the past decade due to benefits, such as low-cost and high-volume manufacturing techniques, thin and bendable structures and environmental friendliness. Autonomous electronic systems [1] are one potential application, which would greatly benefit from low-cost and bendable printed circuits, including both power source and interim energy storage. [2]

Numerous technologies have been developed to provide energy for low power wireless systems. Piezoelectric devices are one way to harvest mechanical energy from ambient sources. Piezoelectric materials have also been used in combination with printing technologies to produce functional components for sensor application. Combining different printing techniques is essential when the components in the circuit differ in terms of their materials and structure. Typically, conducting porous films are desirable in energy storage applications [2], whereas in semiconductor components a thin and homogeneous layer is required.

Recently, piezoelectric polyvinylidene fluoride (PVDF) film sensors with CNT electrodes, printed with a flexographic technique [3, 4], as well as gravure printed organic diodes [5, 6], were reported. Most recently, solution-processable supercapacitors from a CNT dispersion were reported [7, 8]. Here, we combine these previously developed printed components into a circuit, where the supercapacitor is charged with the energy provided by a piezoelectric element excited by low-frequency harmonic motion. As a transducer we used rolled PVDF films and, as a reference, a rigid piezoceramic element. The printed organic diodes were used as a passive rectifying circuit.

In this work we demonstrate an energy harvesting circuit fabricated by mass manufacturing compatible methods. In general, energy harvesting from low-frequency harmonic motion is considered inefficient, since the maximum power depends strongly on the frequency [9]. In this paper we address these challenges in the case of the printed energy harvesting circuit.

II. EXPERIMENTAL

A supercapacitor and organic diodes were fabricated on poly(ethylene terephthalate) (PET) substrate (Melinex ST506 from DuPont). The circuit wiring was 100 nm thick copper deposited by electron beam evaporation through a shadow mask.

A. *Supercapacitor assembly and characterization*

The supercapacitor electrodes were fabricated from CNT / xylan nanocomposite dispersion by a blade coating method, adapted from earlier work [7, 8]. The multi-walled carbon nanotube (MWNT) content was 3.5 wt-% and that of xylan 1.75 wt-%. The electrodes were prepared by coating multiple films on top of each other. The bottom electrode was fabricated on the same substrate with the diodes, and the top electrode was laminated on top (see Fig. 1). The separator film used in the capacitors was TF4050 (Nippon Kodoshi Corp). An adhesive film (UPM Raflatac) was used to attach the electrodes together, and to seal the electrolyte in between. The

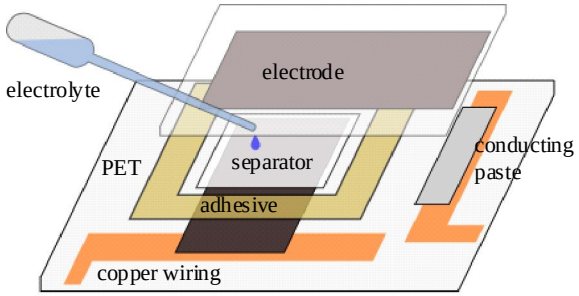

Fig. 1. The structure of assembled supercapacitor.

This work was supported by the Finnish Funding Agency for Technology and Innovation and the Academy of Finland.

J. Pörhönen, S. Lehtimäki and S. Tuukkanen are with the Department of Electronics and Communications Engineering, and S. Rajala with the Department of Automation Science and Engineering, at Tampere University of Technology, 33101 Tampere, Finland (e-mail: sampo.tuukkanen@gmail.com).

electrolyte was a 1 M solution of NaCl in water.

Electrode sheet resistances were studied by four-point measurements. Supercapacitor capacitance and equivalent series resistance (ESR) were determined by galvanostatic discharge measurements according to an international IEC 62391-1 standard, Class 3 ("Power") [10]. Measurements were carried out with Zennium Electrochemical Workstation (Zahner Elektrik GmbH). The supercapacitor was charged from 0 V to 0.9 V with a one minute ramp, then held at 0.9 V for 30 minutes. After this electrification time, the supercapacitor was discharged with a constant current. Supercapacitor capacitance was calculated according to

$$C = -\frac{I}{\mathrm{d}V/\mathrm{d}t}, \quad (1)$$

where *dV/dt* is the voltage decline between 80 % and 40 % of 0.9 V. ESR was calculated from

$$ESR = \frac{\Delta U}{I}, \quad (2)$$

where ΔU is the voltage drop (IR drop) at the beginning of the discharge phase. Here I is the discharging current determined by the selected device class in the standard. Cyclic voltammograms at voltage ramp rates from 5 mV/s to 100 mV/s were also recorded with the Zennium potentiostat. The energy stored in the supercapacitor is

$$E = \frac{1}{2}CV^2, \quad (3)$$

and the maximum power that can be delivered to the load is

$$P = \frac{\mathrm{V}^2}{4 \times ESR}. \quad (4)$$

Here V is the supercapacitor voltage. [11, 12]

B. Rectifying diode circuit

The gravure printing method used to fabricate the diodes was adapted from earlier work [5]. The diodes were used to form a passive rectifier circuit used in voltage doubler configuration [13]. A schematic picture of the circuit is shown in Fig. 2.

On the bottom, the deposited copper layer functioned as the diode cathode. The used semiconductor was 12.5 % poly(triarylamine) (PTAA) obtained in solution from Merck Chemicals Ltd. On top, Acheson Electrodag PM-460A from Henkel was used as the diode anode. The paste ink was diluted

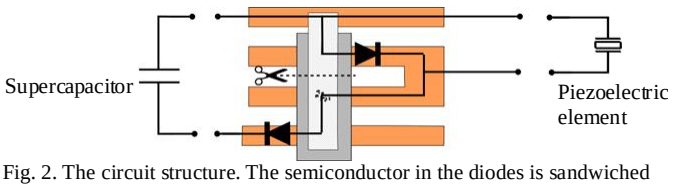

Fig. 2. The circuit structure. The semiconductor in the diodes is sandwiched between copper (cathode) and silver (anode) layers. The silver layer is cut, and the diode in the middle is short-circuited.

TABLE I
TYPICAL PROPERTIES OF 28 µM PVDF MATERIAL [15].

Symbol	Quantity	Value
d_{33}	Piezoelectric coefficient	$-33 \cdot 10^{-12}$ C/N
d_{31}	Piezoelectric coefficient	$23 \cdot 10^{-12}$ C/N
k_{31}	Electromechanical	0.12
k_t	Coupling Factors	0.14
Y	Young's modulus	$2 \cdot 10^9$-$4 \cdot 10^9$ N/m^2
C	Capacitance	380 pF/cm^2
ε	Permittivity	$106 \cdot 10^{-12}$-$113 \cdot 10^{-12}$ F/m
$\varepsilon/\varepsilon_0$	Relative permittivity	12-13
ρ	Mass density	$1.78 \cdot 10^3$ kg/m^3
T	Temperature range	-40 to +80…100 °C

with n-propylacetate to suit gravure printing. The weight ratio of PM-460A to n-propylacetate was 13:1. Diode I-V characteristics were measured with Keithley 236 source-measure unit.

C. Piezoelectric elements

PVDF ($(CH_2\text{-}CF_2)_n$) is a piezoelectric material having a solid structure with approximately 50-65 % crystallinity [14]. In this study 28 µm and 110 µm thick PVDF films (Measurement Specialties, Inc) with screen printed silver ink metallization were used. Table I lists the typical properties of the 28 µm thick PVDF material [15]. A rigid piezoceramic element (round disk, ⌀ 14 mm, on a metal plate) was used as a reference for the PVDF material.

An external force compressing the film generates a charge to appear at the electrodes. PVDF is an anistropic material and thus its electrical and mechanical properties differ depending on the direction of the external force. The generated surface-charge density D is defined by

$$D = \frac{Q}{A} = d_{3n}X_n, \quad (5)$$

where Q is the charge, A is the electrode area, d_{3n} is the piezoelectric coefficient and X_n is the applied stress [15]. The coefficient d_{3n} has two subscripts – the first refers to electrical axis and the second to the mechanical axis defined in Fig. 3. The electrical axis is 3, and the mechanical axis n can be 1, 2 or 3. Typical operation modes for PVDF sheet elements are presented in Fig. 3.

To maximize the charge developed by the mechanical input, the PVDF sheets (size 230 mm × 15 mm) were made into rolls. The sheets were rolled along the mechanical axis 1 to operate both in 33- and 31-modes.

D. Sensitivity measurements

To evaluate the operation, the sensitivities of the

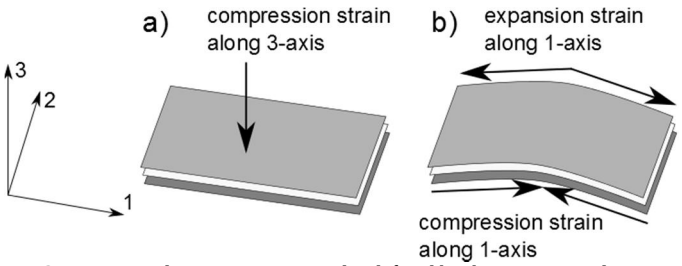

Fig. 3. Two piezoelectric operation modes defined by the conventional axis definition: the 33-mode (a) and the 31-mode (b).

manufactured PVDF rolls were measured. The sensitivity measurement setup, shown in Fig. 4, is presented in detail in Refs. [16] and [3]. Briefly, Brüel & Kjaer Mini-Shaker (Type 4810) was used to provide a dynamic excitation force. A sinusoidal input for the shaker was provided with a Tektronix AFG3101 function generator. The force was measured with a high-sensitivity dynamic force sensor (PCB Piezotronics 209C02) and the PVDF roll output with a custom-made combination of a charge amplifier and a 16-bit AD-converter. The sensitivity is obtained by dividing the PVDF roll output charge with the dynamic force. Thus, the unit of sensitivity is pC/N.

In sensitivity measurements, a static force of 3 N was adjusted to keep the PVDF roll in place. A dynamic excitation force of about 1.3 N and frequency of 2 Hz were used. The sensitivity of each PVDF roll was measured from four points in the middle of the roll and the mean sensitivity value is presented in the results.

E. Energy harvesting setup

According to a quantitative model [17], the efficiency of a piezoelectric energy harvester is

$$\eta = \left(\frac{1}{2}\right)\frac{k^2}{1-k^2} \Big/ \left(\frac{1}{Q_m} + \frac{1}{2} \times \frac{k^2}{1-k^2}\right), \quad (6)$$

where k is the electromechanical coupling coefficient and Q_m is the mechanical quality factor. Additionally, the efficiency increases with decreasing dielectric loss factor (tan δ_d) [18]. All of these parameters depend on frequency, and the best efficiency is achieved at the resonance frequency of the piezoelectric element [19, 20].

In energy harvesting experiments with the Mini-Shaker setup, a sinusoidal control signal was used to achieve harmonic motion at 10 Hz frequency, and both static and dynamic force amplitudes were monitored. For demonstration purposes the piezoelectric elements were also tested by treading the elements by foot with approximately 2 Hz frequency. The energy stored in the supercapacitor was used to switch the state of a printed 10 mm x 10 mm electrochromic display element (Acreo Swedish ICT).

III. Results and Discussion

The thickness of the supercapacitor electrodes was approximately 10 µm, and their sheet resistance 12-14 Ω/sq. The circuit as a whole is shown in Fig. 5.

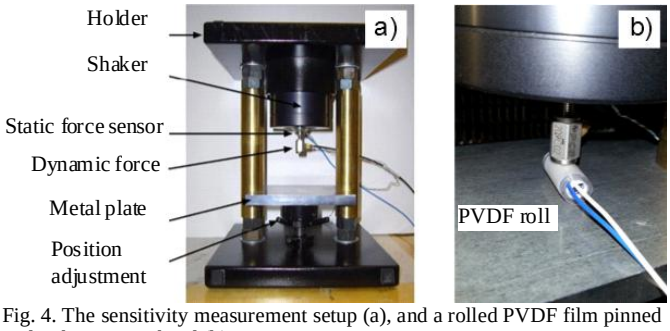

Fig. 4. The sensitivity measurement setup (a), and a rolled PVDF film pinned under the moving head (b).

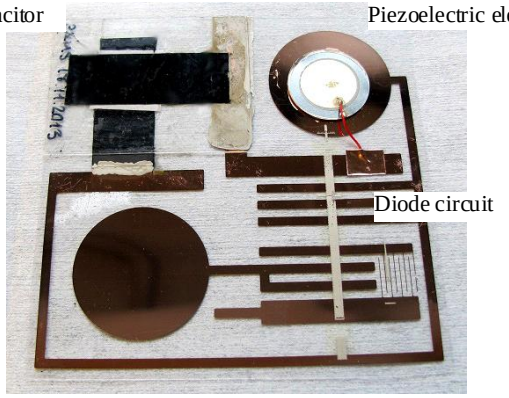

Fig. 5. The integrated energy harvesting circuit prototype with the

The capacitance of the supercapacitor was approximately 20 mF, and ESR was 100 Ω. Cyclic voltammograms, recorded at different ramp rates between 0 V and 0.9 V, are presented in Fig. 6. Their rectangular shape indicates good capacitive behavior.

Diode I-V curves are shown in Fig. 7. It can be seen that the amount of charge delivered to the supercapacitor is negligible when the output voltage generated by the energy source is below 2 Volts. To get the diodes in their conducting state, the piezoelectric element has to provide at least this much voltage. This is a challenge considering energy harvesting in low-force applications, since the surface-charge density in the PVDF films is directly proportional to the applied stress, according to Eq. 5.

The results of the sensitivity measurements are shown in Table II. They revealed remarkably higher sensitivities when compared to the d_{33} coefficient given by the manufacturer ($d_{33} = -33$ pC/N [15]). This is mainly due to the operation also in d_{31}-mode, as well as the structure of the roll: the same force is applied to several locations of the roll simultaneously. The lower sensitivity of the thicker PVDF film is probably due to the stiffer material properties. The sensitivity of the PVDF roll is mainly related to the amount of deformation of the rolled films.

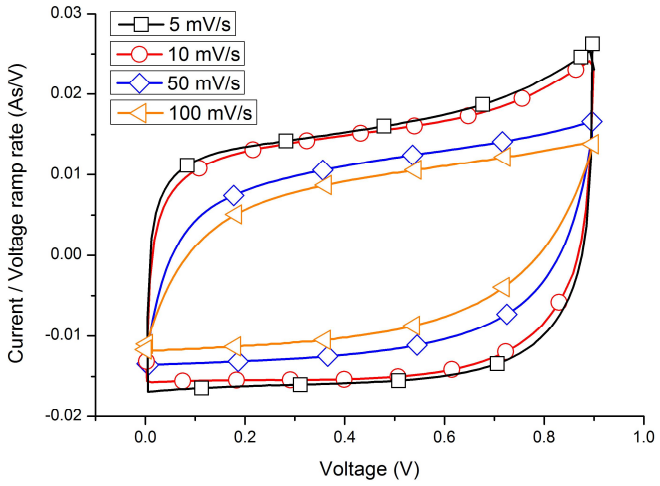

Fig. 6. Supercapacitor cyclic voltammetry (CV) curves.

TABLE II
MEASURED SENSITIVITIES OF THE PVDF ROLLS.

Element	Thickness	Sensitivity
Rolled PVDF films	110 µm	1200 pC/N
(size 230 mm × 15 mm)	28 µm	2800 pC/N
Piezoceramic (⌀ 14 mm)		3700 pC/N

When the piezoelectric elements (listed in Table II) were driven with the Mini-Shaker, the dynamic force was approximately 1–3 N, depending on the signal amplitude from the function generator. This stimulation resulted in much higher charging speed with the piezoceramic element. The supercapacitor charging curves, measured when the elements were driven at 10 Hz frequency, are presented in Fig. 8. The charging curves, measured when the elements were treaded by foot at approximately 2 Hz frequency, are presented in Fig. 9.

The efficiency of energy harvesting depends on the coupling coefficient (k) and the quality factor (Q_m), according to Eq. 6. The coupling coefficient of the used PVDF film (Table I) is significantly smaller than those of piezoceramics (typically 0.5–0.7) [19]. Furthermore, dielectric losses in piezoceramics are practically insignificant (loss factor in a range of 0.002–0.02), whereas the dielectric loss factor of PVDF is approximately 0.25 [21]. It has also been reported that dielectric losses in metallized PVDF films sharply increase with lowering frequency [22].

In comparison to the results obtained with the Mini-Shaker setup, the supercapacitor charging speed with the piezoceramic element was significantly lower in the treading experiment. In contrast, the charging speed obtained with the rolled PVDF film was only reduced by approximately 50%. The sensitivity values presented in Table II were measured from the middle of the PVDF roll. Instead, when measuring from the edge of the roll, higher sensitivity values were obtained (3000–4000 pC/N for the 28 µm film). The higher sensitivity at the edges is probably due to larger bending of the roll. This may also explain the operation in the foot treading measurements: when the PVDF roll was mounted under foot, the roll was flattened completely. These results suggest that

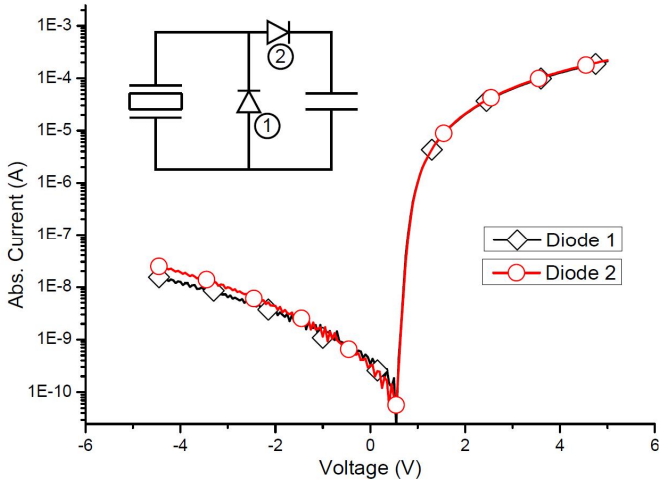

Fig. 7. The diode I-V curves. A schematic of the harvester circuit is shown as inset.

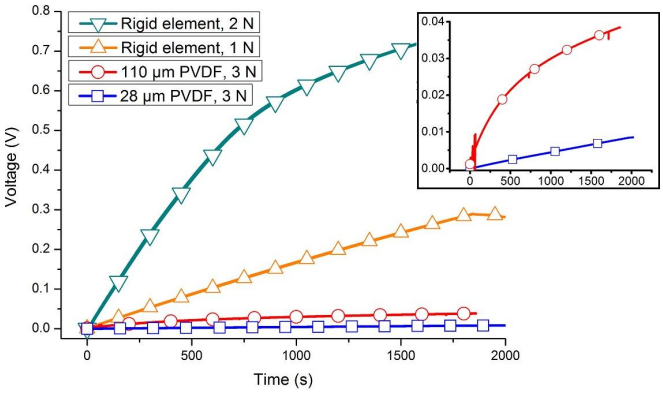

Fig. 8. The capacitor charging curves, when the piezoelectric elements were driven by sinusoidal signal at 10 Hz frequency and low force (1-3 N).

the rolled PVDF sheets are better suited for energy harvesting applications with a sufficiently large displacement. In addition, multiple rolls can be used to multiply the output. [23]

After the supercapacitor was first charged to 0.7 V using the piezoceramic element, the supercapacitor was connected to the electrochromic display, where slow switching occurred. As can be seen from Fig. 10, good contrast was achieved.

The supercapacitor voltage dropped instantaneously when current was drawn, but recovered to a level approximately 50 mV lower than before switching. According to Eq. 3, this translates into 25 µJ energy consumption. The sudden drop is probably related to slow movement of the electrolyte ions in the porous electrodes (high ESR), which restricts the available power, according to Eq. 4. The following recovery of the voltage could be due to charge re-distribution within the device [24].

IV. CONCLUSIONS

In this work we reported a flexible energy harvesting circuit built from printable components, including a supercapacitor, organic diodes and a piezoelectric element, and demonstrated the concept in a practical application. The rolled PVDF film elements gave out considerably higher sensitivity values than the d_{33} value reported by the manufacturer. Despite similar

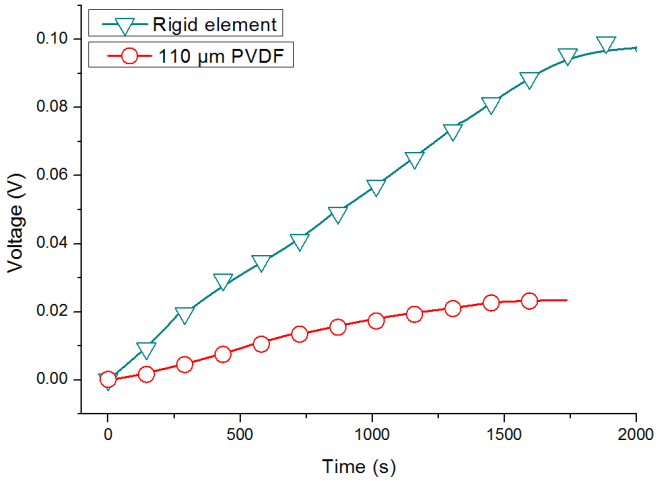

Fig. 9. The capacitor charging curves, when the piezoelectric elements were treaded by foot at approximately 2 Hz frequency.

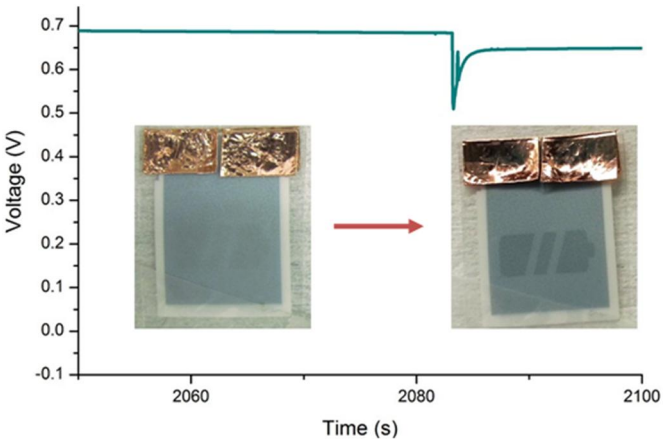

Fig. 10. Supercapacitor voltage during switching and the resulting image on the electrochromic display.

sensitivity values measured for the PVDF rolls and the piezoceramic reference element, the rolls were less effective in harvesting mechanical energy than the rigid ceramic element.

The considerable losses in the energy harvesting stem from two sources. On one hand, the diode I-V characteristics present a challenge, since a relatively high voltage is required to get the diodes in their conducting state. On the other hand, the low coupling coefficient of PVDF and its high dielectric loss factor cause additional losses.

Based on the results from the energy harvesting experiments, the performance of the rolled PVDF films is improved by maximizing the caused distortion. Hence, the rolled PVDF films are better suitable for energy harvesting applications where considerable force is applied. The rolled elements would be also of use in sensory applications, where high sensitivity is required. We showed that the energy harvester can be used in an application where the energy stored to the supercapacitor is used to switch an electrochromic display.

V. Acknowledgement

The authors thank Veijo Kangas from Morphona Ltd. for the preparation of the CNT ink. The authors acknowledge funding from the Finnish Funding Agency for Technology and Innovation (Tekes, Dec. No. 40049/12) and the Academy of Finland (Dec. No. 137669 and 138146).

References

[1] S. Kim et al. (2013, July). No Battery Required: Perpetual RFID-Enabled Wireless Sensors for Cognitive Intelligence Applications. *Microwave Magazine, IEEE*. [Online]. *14(5)*, pp. 66–77. Available: http://ieeexplore.ieee.org/xpls/abs_all.jsp?arnumber=6556093

[2] S. Lehtimäki, M. Li, J. Salomaa, J. Pörhönen, A. Kalanti, S. Tuukkanen, P. Heljo, K. Halonen, D. Lupo. (2014, June). Performance of printable supercapacitors in an RF energy harvesting circuit. *International Journal of Electrical Power & Energy Systems*. [Online]. *58*, pp. 42–46. Available: http://www.sciencedirect.com/science/article/pii/S0142061514000052

[3] S. Tuukkanen, T. Julin, V. Rantanen, M. Zakrzewski, P. Moilanen, K.E. Lilja, and S. Rajala. (2012, Dec.). Solution-processible electrode materials for a heat-sensitive piezoelectric thin-film sensor. *Synthetic Metals*. [Online]. *162(21–22)*, pp. 1987–1995. Available: http://www.sciencedirect.com/science/article/pii/S0379677912003049

[4] S. Tuukkanen, T. Julin, V. Rantanen, M. Zakrzewski, P. Moilanen, and D. Lupo. (2013, May) Low-Temperature Solution Processable Electrodes for Piezoelectric Sensors Applications. *Japanese Journal of Applied Physics*. [Online] *52*. Available: http://jjap.jsap.jp/link?JJAP/52/05DA06

[5] K. E. Lilja, H. S. Majumdar, K. Lahtonen, P. Heljo, S. Tuukkanen, T. Joutsenoja, M. Valden, R. Österbacka and D. Lupo. (2011, Jun.). Effect of dielectric barrier on rectification, injection and transport properties of printed organic diodes. *Journal of Physics D: Applied Physics*. [Online] *44*. Available: http://iopscience.iop.org/0022-3727/44/29/295301

[6] P. Heljo, M. Li, K.E. Lilja, H.S. Majumdar, and D. Lupo. (2013, Feb.). Printed Half-Wave and Full-Wave Rectifier Circuits Based on Organic Diodes. *IEEE Transactions on Electron Devices*. [Online]. *60(2)*, pp. 870–874. Available: ieeexplore.ieee.org/xpls/abs_all.jsp?arnumber=6407991

[7] S. Lehtimäki, J. Pörhönen, S. Tuukkanen, D. Lupo. (2014) Fabrication and characterization of solution processed carbon nanotube supercapacitors. Presented at MRS Fall 2013 Conference Proceedings. [Online]. Available: http://dx.doi.org/10.1557/opl.2014.178

[8] S. Lehtimäki, S. Tuukkanen, J. Pörhönen, P. Moilanen, J. Virtanen, M. Honkanen, D. Lupo. (2014, Jan.). Low-cost, solution processable carbon nanotube nanocomposite supercapacitors and their characterization. *Submitted*. [Online].

[9] P.D. Mitcheson, E.M. Yeatman, G.K. Rao, A.S. Holmes, and T.C. Green. (2008, Sept.). Energy harvesting from human and machine motion for wireless electronic devices. *Proceedings of the IEEE*. [Online]. *96(9)*, pp. 1457–1486. Available: http://ieeexplore.ieee.org/xpls/abs_all.jsp?arnumber=4618735

[10] International standard: Fixed electric double layer capacitors for use in electronic equipment, IEC Standard 62391-1, 2006.

[11] B.E. Conway, Electrochemical supercapacitors: scientific fundamentals and technological applications (POD). New York: Kluwer Academic/plenum, 1999.

[12] R. Kötz and M. Carlen. (2000, May). Principles and applications of electrochemical capacitors. *Electrochimica Acta*. [Online]. *45(15)*, pp. 2483–2498. Available: http://www.sciencedirect.com/science/article/pii/S0013468600003546.

[13] Y.K. Ramadass and A.P. Chandrakasan. (2010, Jan.). An efficient piezoelectric energy harvesting interface circuit using a bias-flip rectifier and shared inductor. *Solid-State Circuits, IEEE Journal of*. [Online]. *45(1)*, pp. 189–204. Available: http://ieeexplore.ieee.org/xpls/abs_all.jsp?arnumber=5357551

[14] G. Eberle, H. Schmidt and W. Eisenmenger, "Piezoelectric polymer electrets", IEEE T Dielect El In, 1996, vol. 3, pp. 624-646.

[15] Measurement Specialties Inc., "Piezo film sensors", available: http://www.meas-spec.com/downloads/Piezo_Technical_Manual.pdf.

[16] S. Kärki, J. Lekkala, H. Kuokkanen and J. Halttunen. (2009, Aug.). Development of a piezoelectric polymer film sensor for plantar normal and shear stress measurements. *Sensors and Actuators A:Physical*. [Online]. 54, p.57-64. Available: http://www.sciencedirect.com/science/article/pii/S092442470900332X

[17] C. D. Richards, M. J. Anderson, D. F. Bahr and R. F. Richards. (2004, Mar.). Efficiency of energy conversion for devices containing a piezoelectric component. *Journal of Micromechanics and Microengineering*. [Online]. *14(5)*. Available: http://iopscience.iop.org/0960-1317/14/5/009

[18] M. Umeda, K. Nakamura, and S. Ueha. (1996, Jan.). Analysis of Transformation of Mechanical Impact Energy to Electrical Energy Using a Piezoelectric Vibrator. *Japanese Journal of Applied Physics*. [Online]. *35(1)*, pp. 3267–3273. Available: http://jjap.jsap.jp/link?JJAP/35/3267/

[19] A. Safari & E. K. Akdogan (eds.), "Piezoelectric Transducer Designs for Sonar Applications," in *Piezoelectric and Acoustic Materials for Transducer Applications, 1st* ed. New York: Springer, 2008, pp. 217-240.

[20] C. Soh, Y. Yang, and S. Bhalla, "Future of Smart Materials," in *Smart Materials in Structural Health Monitoring, Control and Biomechanics, 1st* ed. Berlin: Springer, 2012, pp. 583-594.

[21] A. Puttmer, P. Hauptmann, R. Lucklum, O. Krause, and B. Henning. (1997, Jan.). SPICE Model for Lossy Piezoceramic Transducers. *IEEE Transactions on Ultrasonics, Ferroelectrics, and Frequency Control*. [Online]. 44(1), pp. 60-66. Available: http://ieeexplore.ieee.org/xpls/abs_all.jsp?arnumber=585191

[22] V. S. Yadav, D. K. Sahu, Y. Singh, and D.C.Dhubkarya. (2010, Mar.). The Effect of Frequency and Temperature on Dielectric Properties of

Pure Poly Vinylidene Fluoride (PVDF) Thin Films. Presented at International MultiConference of Engineers and Computer Scientists. [Online]. Available: http://www.iaeng.org/publication/IMECS2010/IMECS2010_pp1593-1596.pdf

[23] K. Ishida, T. C. Huang, K. Honda, Y. Shinozuka, H. Fuketa, T. Yokota, U. Zschieschang, H. Klauk, G. Tortissier, T. Sekitani, H. Toshiyoshi, M. Takamiya, T. Someya, and T. Sakurai. (2013, Jan.). Insole Pedometer With Piezoelectric Energy Harvester and 2 V Organic Circuits. *Solid-State Circuits, IEEE Journal of*. [Online]. 48(1), pp. 255-264. Available: http://ieeexplore.ieee.org/xpls/abs_all.jsp?arnumber=6399549

[24] G. V. Merrett & A. S. Weddell. (2012, June). Supercapacitor leakage in energy-harvesting sensor nodes: Fact or fiction?. *Networked Sensing Systems (INSS), Ninth International Conference on*. [Online]. p. 1-5. Available: http://ieeexplore.ieee.org/xpls/abs_all.jsp?arnumber=6240581

Juho Pörhönen received his M.Sc. in electrical engineering from Tampere University of Technology (TUT), Tampere, Finland in September 2013. During 2012-2013 he worked as a research assistant at the Department of Electronics and Communications Engineering and did his Master's thesis in a research project concerned with printable movement sensors. After graduation he continues to work in project related tasks at the Laboratory for Future Electronics (LFE) at TUT. The main focus of his work is on printable electronics and energy harvesting applications.

Satu Rajala (née Kärki) received her D.Sc. (Tech.) from TUT in 2009 with the thesis “Film-type sensor materials in measurement of physiological force and pressure variables”. She has been working in the Department of Automation Science and Engineering since May 2003. Her research activities include sensor systems for physiological measurements.

Suvi Lehtimäki received her M.Sc. in Chemistry from Tampere University of Technology (TUT) in June 2012. She is currently working towards a doctoral degree at the Laboratory for Future Electronics at TUT. Her research is focused on printable supercapacitors for energy harvesting applications.

Sampo Tuukkanen received his Ph.D. in December 2006 from Department of Physics, University of Jyväskylä (JYU), Finland, with the thesis "Dielectrophoresis as a tool for on-chip positioning of DNA and electrical characterization of nanoscale DNA". In 2007-2009 he did a postdoc in Molecular Electronics Group in CEA/Saclay, France, working on the synthesis and electronic applications of carbon nanotubes (CNT). From May 2009 until February 2014 he worked as a senior scientist in Laboratory for Future Electronics (LFE) at TUT. His current position is in Microfabrication Group, Department of Material Science and Engineering, School of Chemical Technologies, Aalto University, Finland.